SSRG International Journal of Civil Engineering
ISSN: 2348-8352/ https://doi.org/10.14445/23488352/IJCE-V11I5P105

Volume 11 Issue 5, 41-55, May 2024

Original Article

In-Plane Free Vibrations Analysis of Tapered Arches with Variable Radius Using the Rayleigh-Ritz Method

Ahmed BABAHAMMOU[1], Omar Outassafte[2], Soufiane Elouardi[3], Adil Zine[4], Rhali Benamar[5]

[1,3] *SSDIA Laboratory, Hassan II University of Casablanca, ENSET of Mohammedia, Morocco.*
[2] *Laboratory of Mechanics Production and Industrial Engineering (LMPGI), High School of Technology (ESTC), Hassan II University of Casablanca, Oasis, Casablanca, Morocco.*
[4] *Laboratoire de Mécanique de Lille (LML), Université de Lille 1, French.*
[5] *University Mohammed V Rabat, E.M.I. Agdal, Rabat, Morroco.*

[1] *Corresponding Author : ahmedbabahammou@gmail.com*

Received: 04 March 2024 Revised: 06 April 2024 Accepted: 05 May 2024 Published: 31 May 2024

Abstract *- This paper investigates the in-plane free vibrations of thin arches with variable radius and varying cross-sections employing the Rayleigh-Ritz method (RRM). A novel aspect of this study lies in the trial arc functions, which are solutions of the sixth-order differential equation governing the vibration motion of circular arches with constant cross-section. These trial functions are obtained through symbolic computation. Numerical computation is then utilized to determine the eigenvalues, representing frequency parameters, and eigenvectors, representing mode shapes. The investigation considers three different end conditions (clamped-clamped, clamped-simply supported, and supported at both ends) and five arc geometries (parabolic, catenary, spiral, circular, and cycloid) with varying opening angles, taper types, and taper ratios. The convergence study highlights the sensitivity of the results to the taper ratio, with convergence rates faster than those observed in previous RRM studies. Frequency parameters are accurately calculated and compared favourably with existing literature. Additionally, mode shapes are plotted, demonstrating the significant influence of the taper ratio on mode shapes.*

Keywords *- In-plane vibrations, Rayleigh-Ritz method, Thin arches, Variable radius, Varying cross-section, Trial arc functions, Eigenvalues, Eigenvectors, Taper ratio, Mode shapes.*

1. Introduction

In civil Fields, the arches give excellent structural function and beautiful appearances. For example, the horseshoe arc is used to frame structures [19]; in mechanical, they convert the bending load into a compressive force to give the structure good rigidity; in aerospace, they can model the scimitar rotor blades [2], they are also essentials in many other fields: sensors, piping systems, roof structures, bridges, and aerospace structures, etc. In particular, arches with variable sections and curvature make it possible to optimize the material choice and control the force distribution uniformity. Consequently, much literature has been published on the in-plane vibration of these arches. Much work had been done on the vibration of many types of arches during the 19th th century after, Rayleigh proposed the trial arc functions containing an undermined exponential parameter allowing the optimization of the frequency parameters. Laura et al. studied the circular arc with varying cross-sections by the Rayleigh-Ritz Method (RRM) using the same set of trial functions [21, 16]. Romanelli [22] and Wang [25] investigated clamped and hinged non-circular arches; they used the Rayleigh-Ritz Method by taking as trial functions sin functions satisfying the end conditions. Gutierrez [12] and Rossi [23] employed the Ritz Method by means of polynomial coordinate functions to study tapered arches with varying curvature. The same arc type has been studied by Huang [13] and Tang using the so-called exact solutions.

Byoung [18] used his calculation of the Cartesian coordinates instead of the polar coordinates to study the free vibration of parabolic arches. Liu [20] used the accurate generalized differential quadrature rule, and Karami [15] used the differential quadrature method. Shin [24] applied the Generalized Differential Quadrature Method (GDQM) and Differential Transformation Method (DTM) to vibration analysis of circular arches with variable cross-sections. Author dealt with the in-plane free vibration of circular arches with variable cross-sections by means of the exact solution. An authour investigated the dynamic response of circular arches with variable cross-sections subjected to seismic ground motions. Adair [2] studied the free in-plane vibrations of rotating arches with a variable cross-section using the so-called Adomian Modified Decomposition

Method (AMDM). Noori used the Complementary Functions Method (CFM) to investigate the in-plane free and forced vibration responses of axially functionally graded parabolic tapered arches. Wang derived the differential equations of motion of the in-homogeneous tapered arches with variable curvature under elastic constraints [26]. Melchiorre investigated elastic tapered arches with variable curvature using differential formulation and numerical solution.

As is well known, the RRM is a simple and systematic way to find frequency parameters and associated mode shapes of various structures such as plates, shells and arches. It makes it possible to solve problems with several complexities, such as the existence of added masses, the supports of the studied structures on point [6] or distributed elastic supports [7], for isotropic, orthotropic or in-homogeneous materials, FGM, etc. It is especially used for introduction to the study of nonlinear vibrations by Benamar's method. However, the major problem of the RRM is the choice of the trial functions. Indeed, Laura et al. [23, 17, 16, 12, 9, 11] studied the vibrations of arches with variable radius and section, with added masses, and elastically restrained at ends using the RRM. Unfortunately, the calculation presents an instability problem, and the accuracy of the method concerns only shallow arches [3] due to the set of trial arc functions, which are polynomial functions with an exponential optimization parameter.

It is well known that the set of the trial functions used in RRM must satisfy the following conditions: 1) be independent and complete, 2) satisfy the end conditions 3) preferably, must be representative of the studied arc. This third condition is not imperative, but if it is not respected, the calculation time is likely to be significant, and the convergence is slow. This paper proposes a precise RRM giving arc good results and having a rapid convergence in order to study arcs of variable sections (called tapered arcs) and variable curvature. The choice of the trial arc functions is the method's strong point; they are taken as a particular solution of the differential equation governing the in-plane arc vibrations corresponding to an opening angle $= 1\ rad$. The set of this trial functions is independently complete and satisfies the end conditions. However, it is based on the arc with constant radius and section: the arc geometric type and the cross-section nature are not involved at this stage. These parameters are considered in the kinetic and the strain energies. Fortunately, computation time and convergence are not affected when this set of trial functions is used to study the frequency parameters and mode shapes of tapered arcs with variable radii.

The present formulation is based on two main steps: the determination of the trial arc functions and the formulation of the Rayleigh-Ritz Method.

1. For the first step, i.e., the determination of the trial arc functions, the arc is supposed to be circular with a uniform section. Indeed, the set of this function must only verify the end conditions of the studied arc. Consequently, the sixth-degree differential equation, which governs the in-plane arc vibrations, becomes with constant coefficients whose solution is relatively less difficult; the author and his co-author resolved this in [4, 8, 5, 1]. Using the end conditions, the symbolic calculation is applied to obtain a system of six equations and seven unknowns, which are the six integration constants and the frequency parameter. Thus, the system matrix is established, and stating its nullity, several frequency parameters are determined, as well as the six associated integration constants. The solutions found constitute the set of the trial arc functions.
2. In the second step, the opening angle, the ratio of the shape of the tapered and the geometric nature of the arc are taken into account. All these parameters are considered to calculate the strain and kinetic energies. The general terms of the dimensionless rigidity and mass matrix are involved. The application of Hamilton's principle gives the Rayleigh-Ritz formulation. The problem is thus reduced to a simple eigenvalue problem easily solvable by Matlab software. For both calculation steps, the arc axis is assumed to be inextensible, rotational inertia and shear deformation effect are neglected, and the arc is assumed to be thin. This formulation of RRM saved us from dealing with a differential equation of sixth degree with variable coefficients and from dealing only with a differential equation of the same order but with constant coefficients. The frequency parameters are found and well compared with those available in the bibliography for several opening angles, shapes and ratios of arc tapered and for the arc geometric nature arc. The modes are also plotted.

The end conditions considered in this work are clamped (C) and supported (S) for five types of arc geometry: parabolic, catenary, cycloid, circular and spiral. Different natures of tapered arcs have been investigated with many functions defining the variation law of the cross-section, and several opening angles were used. For the first time, the results of tapered circular arches are given; after the tapered arches with varying curvature are investigated, the comparison with the bibliography is excellent.

2. General Formulation

2.1. Arc Presentation

The studied arc, shown in Figure 1, is supposed to be homogeneous and thin. Its geometric characteristics are the opening angle θ, the variable radius R, the rectangular cross-section of constant width b and, the variable height h and the variable second moment of inertia with respect to the neutral line of the cross-sectional area $I = \frac{bh^3}{12}$. These three geometric parameters are functions of the curvilinear

abscissa α. The mechanical characteristics of the studied arc, i.e. Young's modulus E and the mass per unit length of the material, μ are supposed to be constant. u The radial and the tangential v displacement, at any point $P(\alpha)$ in the central axis defined by its curvilinear abscissa α, are related by [3]:

$$u(\alpha) = \frac{\partial v(\alpha)}{\partial \alpha} \tag{1}$$

Equation (1) expresses the in-extensibility of the arc axis. The tangential displacement of a current point in the arc axis $\mathrm{v} = \mathrm{v}(\alpha, t)$ is considered harmonic, t being the time. It is assumed to be expressed in the form of a finite series:

$$\mathrm{v}(\alpha, t) = v(\alpha)\sin(\omega t) = a_i v_i(\alpha)\sin(\omega t) \quad i = 1,2\ldots N \tag{2}$$

The repeated index means the Einstein index ω_i is the natural frequency, a_i is an unknown coefficient of the i^{th} trial arc function v_i , and N is the number of the trial arc functions investigated in the next subsection and plotted in Figure 1.

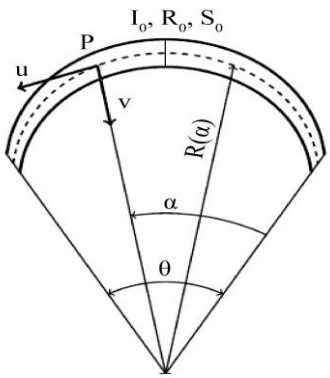

Fig. 1 A tapered arc with variable radius

2.2. Research of Trial Arc Functions

The purpose of this section is to determine a set of trial arc functions that will be used in the current Rayleigh-Ritz formulation.

The basic sixth-order differential equation of the arc in-plane vibration of a current point $P(\alpha)$ in terms of the tangential displacement u is [24, 25]:

$$v^{(6)}(\alpha) + 2v^{(4)}(\alpha) + \left(1 - \frac{\mu S(\alpha)R^4(\alpha)}{EI(\alpha)}\right)v^{(2)}(\alpha) + \frac{\mu S(\alpha)R^4(\alpha)}{EI(\alpha)}v(\alpha) = 0 \tag{3}$$

Where $v^{(n)}(\alpha)$ indicates the n^{th} derivative of the tangential displacement $v(\alpha)$, with respect to α. This equation has non-constant coefficients since the radius and the section are variable. It is well known that the trial arc functions should be orthogonal and verify the arc end conditions. However, they do not necessarily have to constitute a solution of the differential equation expressed in Equation (3). Think of the coefficients in the last equation as constants; it becomes:

$$\begin{aligned} v^{(6)}(\alpha) + 2v^{(4)}(\alpha) + (1 - \bar{\Omega}^2)v^{(2)}(\alpha) + \bar{\Omega}^2 v(\alpha) &= 0 \\ \Omega = \sqrt{\frac{\mu S_0 R_0^4}{EI_0}}\omega & \end{aligned} \tag{4}$$

$\bar{\Omega}$ It is not a frequency parameter of the studied arc. However, it is only a frequency parameter in this very particular case: the arc opening angle $\theta = 1rad$, the radius $R = R_0$ and the height $h = h_0$ are supposed to be constant. This frequency parameter is used to facilitate the determination of the trial arc functions given below.

According to what has been said, the set of trial arc functions deduced from Equation (4) with constant coefficients remains valid for Equation (3) with variable coefficients, even if the individual trial function does not consider the variations of the radius and the section, they will be verified by the series expressed in Equation (2). The variations of the radius and the cross-section are taken into account in the energy study developed in section (?). The general solution of the differential Equation (4) leads to the tangential displacement; it is given by:

$$\begin{aligned} v(\alpha) = \; & C_1\sinh(\lambda_1\alpha) + C_2\cosh(\lambda_1\alpha) + C_3\sin(\lambda_2\alpha) \\ & + C_4\cos(\lambda_2\alpha) + C_5\sin(\lambda_3\alpha) + C_6\cos(\lambda_3\alpha) \end{aligned} \tag{5}$$

In which

$$\begin{aligned} \lambda_1 &= \sqrt{2\sqrt{\frac{p}{3}}\cos\left(\frac{1}{3}\arccos\left(\sqrt{\frac{27q^2}{4p^3}}\right)\right) - \frac{2}{3}} \\ \lambda_2 &= \sqrt{-2\sqrt{\frac{p}{3}}\cos\left(\frac{2\pi}{3} - \frac{1}{3}\arccos\left(\sqrt{\frac{27q^2}{4p^3}}\right)\right) + \frac{2}{3}} \\ \lambda_3 &= \sqrt{-2\sqrt{\frac{p}{3}}\cos\left(\frac{2\pi}{3} + \frac{1}{3}\arccos\left(\sqrt{\frac{27q^2}{4p^3}}\right)\right) + \frac{2}{3}} \\ p &= \frac{1}{3} + \bar{\Omega}^2, \quad q = \frac{2}{27} - \frac{5}{3}\bar{\Omega}^2 \end{aligned} \tag{6}$$

Equation (1) allows to obtain the expression of the radial displacement:

$$\begin{aligned} u(\alpha) = \; & C_1\lambda_1\cosh(\lambda_1\alpha) + C_2\lambda_1\sinh(\lambda_1\alpha) + C_3\lambda_2\cos(\lambda_2\alpha) \\ & - C_4\lambda_2\sin(\lambda_2\alpha) + C_5\lambda_3\cos(\lambda_3\alpha) - C_6\lambda_3\sin(\lambda_3\alpha) \end{aligned}$$

The integration constants C_1 to C_6 are determined by the following end conditions [3, 17]:

$$\begin{aligned} &At\ the\ clamped\ ends \quad v = v^{(1)} = v^{(2)} = 0 \\ &At\ the\ simply\ supported\ ends \quad v = v^{(1)} = v^{(3)} = 0 \end{aligned} \tag{8}$$

The two end conditions at $\alpha = 0$ and $\alpha = \theta$ having three equations each, and described by Equation (8), lead to a system of six equations and seven unknowns, which are the integration constants C_1 to C_6 and the frequency parameter $\bar{\Omega}$. The obtained system can be written as follows:

$$[S].\{C\} = [0] \tag{9}$$

In which $\{C\}$ is a column vector whose components are the six unknown integration constants C_1 to C_6 , i.e., $\{C\}^T = (C_1 \quad C_2 \quad C_3 \quad C_4 \quad C_5 \quad C_6)$ and $[S]$ is a 6×6 square matrix determined by a symbolic calculation. The solutions of the parameter $\bar{\Omega}$ are deducted by imposing the nullity of the determinant of the previous matrix. This leads to a transcendental equation solved numerically by MatLab software to get the series of the frequency parameters $\bar{\Omega}$ described by Eq (4) and corresponding to the end conditions considered. Table 1 gives the first ten frequency parameters $\bar{\Omega}_i$, ($i = 1$ to 10) found for an arc supported at both ends (SS), an arc supported at an end and clamped at the other end (SC), and an arc clamped at its two ends (CC) with an opening angle $\theta = 1rad$. The corresponding normalized tangential $v_i(\alpha^*)$ and radial modes $u_i(\alpha^*)$, described by Equations (5) and (7), are plotted in Figure 2 for SS, SC and CC arches; the dimensionless abscissa $\alpha^* = \frac{\alpha}{\theta}$ varies from 0 to 1. For clarity, only four modes are depicted in Figure 5. It is noticed that the traced modes verify the end conditions, i.e. at the clamped and supported ends, u the tangential and v the radial modes are zero. In contrast, the radial modes v have zero slopes at the clamped ends and have an inflexion point at the supported ends. Even if the found set of the trial functions is based on a circular arc with constant cross-section whose in-plane vibrations are governed by the differential equation with constant coefficients expressed in Equation (4), they constitute the three sets of basic functions used in the present Rayleigh-Ritz formulation. It is applied to the different values of the opening angle θ, for the geometric nature of different arches and many functions defining the change in height $h(\alpha)$.

Table 1. First ten frequency parameters $\bar{\Omega}_i$ obtained for SS, SC and CC circular arches with an opening angle $\theta = 1rad$ and uniform section

	$\bar{\Omega}_1$	$\bar{\Omega}_2$	$\bar{\Omega}_3$	$\bar{\Omega}_4$	$\bar{\Omega}_5$	$\bar{\Omega}_6$	$\bar{\Omega}_7$	$\bar{\Omega}_8$	$\bar{\Omega}_9$	$\bar{\Omega}_{10}$
SS	42.41	85.39	160.88	243.51	358.31	480.45	634.67	796.31	989.14	1177.07
SC	53,22	98,68	181,95	266,99	389,39	513,94	675,71	840,61	1007,01	1149,85
CC	65.72	112.46	204.69	291.05	422.16	548.03	718.45	883.93	1094.16	1320.24

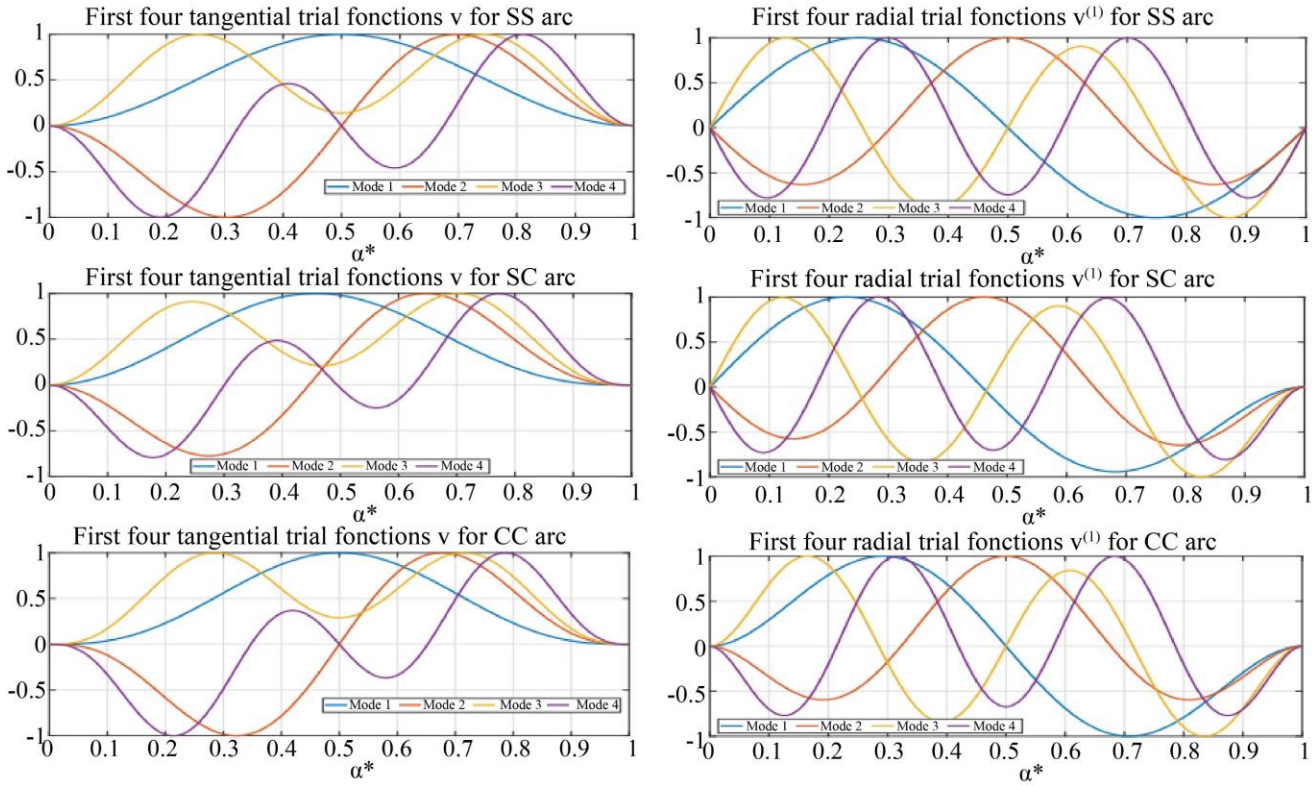

Fig. 2 First four tangential and radial displacements of an arc with an opening angle θ=1rad for CC, CS, and SS end conditions

Table 2. The five values of the integer n define the geometric nature of the studied arches

n	-3	-2	-1	0	1
Nature	Parabola	Catenary	Spiral	Circle	Cycloid

2.3. Rayleigh-Ritz Formulation

Under the assumption of neglected the rotational inertia, the kinetic energy $\boldsymbol{T}$ and the bending strain energy $\boldsymbol{V}$ are given by [12, 14]:

$$\boldsymbol{T} = \frac{1}{2}\mu \int_0^{\theta} \boldsymbol{R}(\alpha)\boldsymbol{S}(\alpha)\left(\left(\frac{\partial \mathbf{v}}{\partial t}\right)^2 + \left(\frac{\partial \mathbf{v}^{(1)}}{\partial t}\right)^2\right) d\alpha \qquad (10)$$

$$\boldsymbol{V} = \frac{1}{2}\boldsymbol{E}\int_0^{\theta} \frac{\boldsymbol{I}(\alpha)}{\boldsymbol{R}^3(\alpha)}\left(\mathbf{v}^{(3)} + \mathbf{v}^{(1)} - \frac{\boldsymbol{R}^{(1)}(\alpha)}{\boldsymbol{R}(\alpha)}\left(\mathbf{v}^{(2)} + \mathbf{v}\right)\right)^2 d\alpha$$

The variation function of the height of the cross-sections $h(\alpha)$ and that of the arc radius $R(\alpha)$ are defined as follows:

$$\begin{aligned} h(\alpha) &= h_0 f(\alpha) \\ R(\alpha) &= R_0 \cos^n(\alpha) \end{aligned} \qquad (11)$$

Where h_0 and R_0 are the height and the radius, respectively, in the middle line $(\alpha = \frac{\theta}{2})$, f is a known function defining the law of the height variation and n is an integer defining the geometric nature of the arc, as shown in Table 2. With due regard for Equations. (2), (10) and (11), the kinetic and the bending strain energies are discretized as follows:

$$\begin{aligned} T &= \frac{1}{2}\omega^2 a_i a_j m_{ij}\cos^2(\omega t) = \frac{1}{2}\omega^2\{A\}^T[M]\{A\}\cos^2(\omega t) \\ V &= \frac{1}{2}a_i a_j k_{ij}\sin^2(\omega t) = \frac{1}{2}\{A\}^T[K]\{A\}\sin^2(\omega t) \end{aligned} \qquad (12)$$

Where $\{A\}$ is an unknown contribution coefficient vector such as $\{A\}^T = \{a_1 \quad a_2 \quad \dots a_N\}$. $[M]$ and $[K]$ are the mass and the linear rigidity matrices, respectively; their general terms are expressed by:

$$\begin{aligned} m_{ij} = \quad & \mu R_0 S_0 \int_0^{\theta} f(\alpha)\left(v_i v_j + v_i^{(1)} v_j^{(1)}\right)\cos^n(\alpha) d\alpha \\ k_{ij} = \quad & \frac{EI_0}{R_0^3}\int_0^{\theta} f^3(\alpha)\left(v_i^{(3)} + v_i^{(1)} - \left(v_i^{(2)} + v_i\right)n\tan(\alpha)\right) \times \\ & \left(v_j^{(3)} + v_j^{(1)} - \left(v_j^{(2)} + v_j\right)n\tan(\alpha)\right)\cos^{-3n}(\alpha) d\alpha \end{aligned} \qquad (13)$$

Hamilton's principle governs the free tapered arc vibrations:

$$\delta \int_0^{\frac{2\pi}{\omega}} (V - T) dt = 0 \qquad (14)$$

The integration of the energies over the range $\left[0, \frac{2\pi}{\omega}\right]$and calculation of the derivatives with respect to the a_i's lead to the tangential dimensional displacement equation whose expression is:

$$2[K]\{A\} - 2\omega^2[M]\{A\} = \{0\} \qquad (15)$$

Equation (15) holds the mechanical and geometric properties of the arc, i.e. the opening angle θ, the material density μ, etc., so that the results are not exploitable on a large scale.

To simplify the study of the influence of geometrical and mechanical parameters on the arc linear behavior, the numerical treatment of the linear algebraic Equation (15) has to be written by a dimensionless expression. Therefore, the following dimensionless parameters are defined:

$$\alpha^* = \frac{\alpha}{\theta} \quad : \text{ The dimensionless angular abscissa}$$

$$v_i^*(\alpha^*) = \frac{v_i(\alpha)}{R_0} \quad : \text{ The dimensionless tangential displacement}$$

$$m_{ij}^* = \frac{m_{ij}}{\mu R_0 S_0} \quad : \text{ The dimensionless mass matrix}$$

$$k_{ij}^* = \frac{R_0^3}{EI_0}.k_{ij} \quad : \text{ The dimensionless rigidity matrix}$$

R_0, h_0, $S_0 = bh_0$ and $I_0 = \frac{bh_0^3}{12}$ are the radius, the thickness, the section area and the second moment of inertia, respectively, at the arc top $\left(\alpha = \frac{\theta}{2}\right)$. It leads to the dimensionless frequency parameter Ω to be found in what follows:

$$\Omega = \sqrt{\frac{\mu S_0 R_0^4}{EI_0}}\omega \qquad (16)$$

Equation(15) then becomes:

$$2[K^*]\{A\} - 2\Omega^2[M^*]\{A\} = \{0\} \qquad (17)$$

$[M^*]$ and $[K^*]$ are the dimensionless mass and rigidity matrices defined by their general terms in which the functions F, G_1, G_2, H_1, H_2 have been generated as follows:

$$\begin{aligned} F(\alpha^*) &= n\tan(\alpha^*) \\ G_1(\alpha^*) &= \cos^n(\alpha^*)G_2(\alpha^*) = \cos^{-3n}(\alpha^*) \\ H_1(\alpha^*) &= F(\alpha^*) \times G_2(\alpha^*)H_2(\alpha^*) = F^2(\alpha^*) \times G_2(\alpha^*) \end{aligned}$$

$$
\begin{aligned}
m_{ij}^{*} &= \theta \int_0^1 G_1(\alpha^*) f(\alpha^*) v_i^* v_j^* d\alpha^* + \frac{1}{\theta} \int_0^1 G_1(\alpha^*) f(\alpha^*) v_i^{*(1)} v_j^{*(1)} d\alpha^* \\
k_{ij}^{*} &= \frac{1}{\theta^5} \int_0^1 G_2(\alpha^*) f(\alpha^*) v_i^{*(3)} v_j^{*(3)} d\alpha^* + \frac{1}{\theta^3} \int_0^1 H_2(\alpha^*) f(\alpha^*) v_i^{*(2)} v_j^{*(2)} d\alpha^* \\
&+ \frac{1}{\theta} \int_0^1 G_2(\alpha^*) f(\alpha^*) v_i^{*(1)} v_j^{*(1)} d\alpha^* \\
&+ \theta \int_0^1 H_2(\alpha^*) f(\alpha^*) v_i v_j d\alpha^* + \int_0^1 H_1(\alpha^*) f(\alpha^*) \left(v_i^{*(1)} v_j^* + + v_j^{*(1)} v_i^* \right) d\alpha^* \\
&+ \frac{1}{\theta} \int_0^1 H_2(\alpha^*) f(\alpha^*) \left(v_i^{*(2)} v_j + v_j^{*(2)} v_i \right) d\alpha^* \\
&+ \frac{1}{\theta^2} \int_0^1 H_1(\alpha^*) f(\alpha^*) \left(v_i^{*(3)} v_j + v_j^{*(3)} v_i \right) d\alpha^* \\
&+ \frac{1}{\theta^3} \int_0^1 G_2(\alpha^*) f(\alpha^*) \left(v_i^{*(1)} v_j^{*(3)} + v_j^{*(1)} v_i^{*(3)} \right) d\alpha^* \\
&\frac{1}{\theta^4} \int_0^1 H_1(\alpha^*) f(\alpha^*) \left(v_i^{*(3)} v_j^{*(2)} + v_j^{*(3)} v_i^{*(2)} \right) d\alpha^*
\end{aligned}
\tag{18}
$$

Equation (17) stands for the Rayleigh-Ritz dimensionless formulation of the linear arc vibration; it is a simple linear algebraic system. The N eigenvalues Ω_i and the eigenvectors associated, which are the contribution coefficient vectors $\{A\}$ expressed by Equation (12), are found numerically using MatLab software. The components a_i of these eigenvectors allow us to calculate the mode shapes expressed in Equation (5),

3. Numerical Results and Discussion

The descriptive analysis has been implemented in MatLab software where a computer code has been written to calculate numerically the dimensionless frequency parameters $\Omega = R_0^2 \sqrt{\frac{\mu S_0}{E I_0}} \omega$ and their associated mode shapes by solving Equation (?). Remember that R_0, S_0 and I_0 are the radius, the area and the second moment of inertia of the cross-section of the arc, respectively, at the axis middle ($\alpha = \frac{\theta}{2}$). The validation of this implementation has been done by comparing the calculated results with those obtained by different methods of solving the same problem. This validation is reported in subsection (3.2). The geometric parameters considered are the opening angle θ, the taper ratio η, the arc geometric nature as displayed in Table 3 and the taper type as shown in Figure 3. η being the tapered ratio. The influence of the variation of the cross-section and the arc geometry on the solution convergence is studied in the next subsection. Five laws for varying the height of the arches shown in Figure 4 are studied.

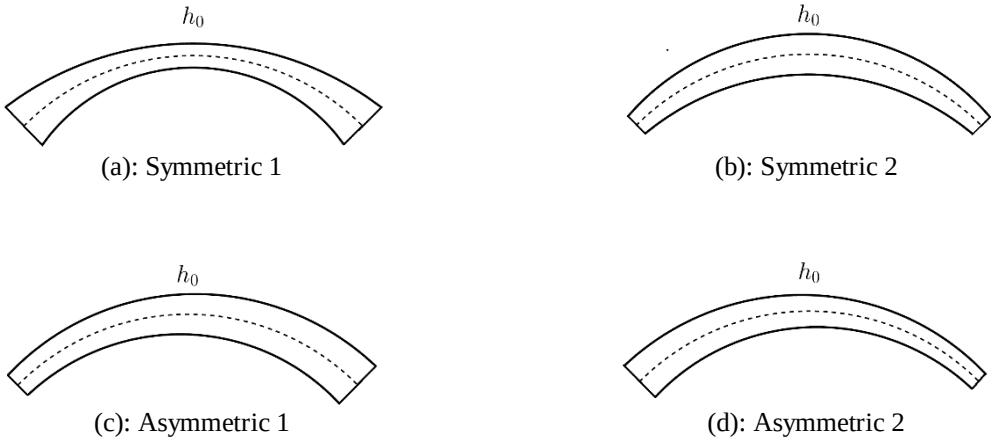

(a): Symmetric 1 (b): Symmetric 2

(c): Asymmetric 1 (d): Asymmetric 2

Fig. 3 Variable cross-section of investigated arches

Case	Arc Shape	The Height Variation Law	
1	Symmetric	$h_1(\alpha^*) = (1 - \eta(2\alpha^* - 1))$	$0 < \alpha^* < 0.5$
		$h_1(\alpha^*) = (1 + \eta(2\alpha^* - 1))$	$0.5 < \alpha^* < 1$
2	Asymmetric 1	$h_2(\alpha^*) = (1 + \eta(2\alpha^* - 1))$	$0 < \alpha^* < 1$
3	Asymmetric 2	$h_3(\alpha^*) = (1 - \eta(2\alpha^* - 1))$	$0 < \alpha^* < 1$
4	Quadratic	$h_4(\alpha^*) = (1 + \eta(2\alpha^* - 1))^2$	$0 < \alpha^* < 1$
5	Symmetric 2 : Sin	$h_5(\alpha^*) = (1 - \eta(sin(\pi\alpha^*) - 1))$	$0 < \alpha^* < 1$

Fig. 4 Five Laws for Varying the Height of the Arches

3.1. Convergence Study

To check the convergence of the first four frequency parameters Ω_i of tapered asymmetric CC arches, the normalized relative deviations are defined as follows:

$$\Delta_i = \frac{\Omega_i - \Omega_P}{\Omega_P} \times 100 \quad i = 1 \ \ to \ \ 4 \tag{19}$$

In which Ω_i is the i^{th} frequency parameter calculated for several values of the number of the trial arc functions $N = 4,5,\ldots$ and Ω_P is the same i^{th} frequency parameter, but calculated from the value P which is the maximum value of N: $P = Max(N)$. These normalized relative differences Δ_i are calculated and plotted as a function of N two cases: by varying the taper ratio and by varying the geometric nature of the arc. For the first convergence study, the arc under consideration (illustrated in Figure 5(d)) is a CC tapered circular; it has an opening angle $\theta = 120°$, and the height variation is the "case 3" type.

Figure 6 gives the curves of convergence study for the first four frequency parameters Ω_i $i = 1$ to 4, according to an integer N with five values of the tapered ratio $\eta = 0,0.1,0.2,0.3,0.4$. These curves allow us to conclude, in a general way, that the convergence is fast and for $N = 7$ these normalized relative differences verify $\Delta_i \leq 0.5\%$ for the lowest four frequency parameters Ω_i. The second remark that can be drawn from these curves is that the tapered ratio decreases the convergence rapidity. Fortunately, this effect is small. The tapered ratio influence on the convergence is explained by the fact that the trial arc functions used in the present Rayleigh-Ritz Formulation are calculated on the basis of an arc with a constant section, so when the section varies (η increases), the calculation program needs more trial arc functions (N increases). The second convergence study concerns $60°$ CC arches (asymmetric 2, "case 3") for five types of arc geometric nature: cycloid, circular, spiral, catenary, and parabola, corresponding to $n = 1,0,-1,-2,-3$, respectively, n being the integer defining the arc geometric nature given in Table 3. The convergence study for the first four frequency parameters Ω_i $i = 1$ to 4, according to the integer, N is summarized in Figure 7. Also, this figure allows us to conclude, in a general way, that the convergence is fast and for $N = 6$ the normalized relative differences $\Delta_i \leq 1\%$ for the lowest four frequency parameters Ω_i and the cited five types of arc geometric nature.

The second remark that can be noticed from these curves is that the convergence rapidity is inversely proportional to the absolute value of $n$the fastest convergence for circular arches ($n = 0$); the convergence studies for a cycloid arc ($n = 1$) and a spiral arc ($n = -1$) are almost identical. The slow convergence is that of the parabola arc ($n = -3$).

Indeed, this was expected; the influence of the arc's geometric nature on the convergence is explained by the fact that the arc trial functions used in the present Rayleigh-Ritz formulation are calculated on the basis of a circular arc. As a result, when the absolute value of the integer defining the geometric nature of the arc n increases, the calculation program requires more trial arc functions (N increases).It can be concluded that the convergence of the Rayleigh-Ritz formulation, presented here, is less sensitive to the variation of the radius. It is seen that using more than 7 arc trial functions will yield normalized relative differences $\Delta \leq 0.01\%$ for CC circular arc and $\Delta \leq 0.4\%$ for parabolic arc respectively.To study higher order convergence, a 30Â° CC parabola arc with a tapered ratio $\eta = 0.4$ is studied. Table 3 gives the convergence of the solution up to the eighth order for a number of test functions varying from 8 to 11. This table shows that, in the worst case, the eighth frequency parameter converges easily for N=11

Table 3. Convergence study for a 30° CC parabola tapered arc with η=0.4

	Ω_1	Ω_2	Ω_3	Ω_4	Ω_5	Ω_6	Ω_7	Ω_8
N=8	198.829	363.593	650.627	953.221	1385.620	1889.660	2667.659	8199.810
N=9	198.763	363.180	649.329	947.565	1364.835	1815.892	2424.949	3179.051
N=10	198.748	363.096	649.097	946.650	1361.689	1804.421	2388.641	3107.409
N=11	198.732	363.062	649.013	946.576	1361.651	1804.410	2388.230	3086.101

For example, for a 20° CS parabola tapered arc ("case 3") with $\eta = 0.4$ and for $N = 8$ trial arc functions, the first eight frequency parameters Ω_i and their contribution coefficients a_i are summarized in Table 4. The arc vibration modes can be easily computed using Equation (2), the lower ones are written as:

$$\begin{aligned} mode\ 1,\quad v(\alpha) = {} & 0.9861v_1(\alpha) + 0.1597v_2(\alpha) + 0.0439v_3(\alpha) + 0.0076v_4(\alpha) \\ & +0.0045v_5(\alpha) + 0.0010v_6(\alpha) + 0.0008v_7(\alpha) + 0.0001v_8(\alpha) \\ mode\ 2,\quad v(\alpha) = {} & 0{,}3772v_1(\alpha) - 0{,}8615v_2(\alpha) - 0{,}3334v_3(\alpha) - 0{,}0569v_4(\alpha) \\ & -0{,}0327v_5(\alpha) - 0{,}0064v_6(\alpha) - 0{,}0053v_7(\alpha) - 0{,}0007v_8(\alpha) \end{aligned} \tag{20}$$

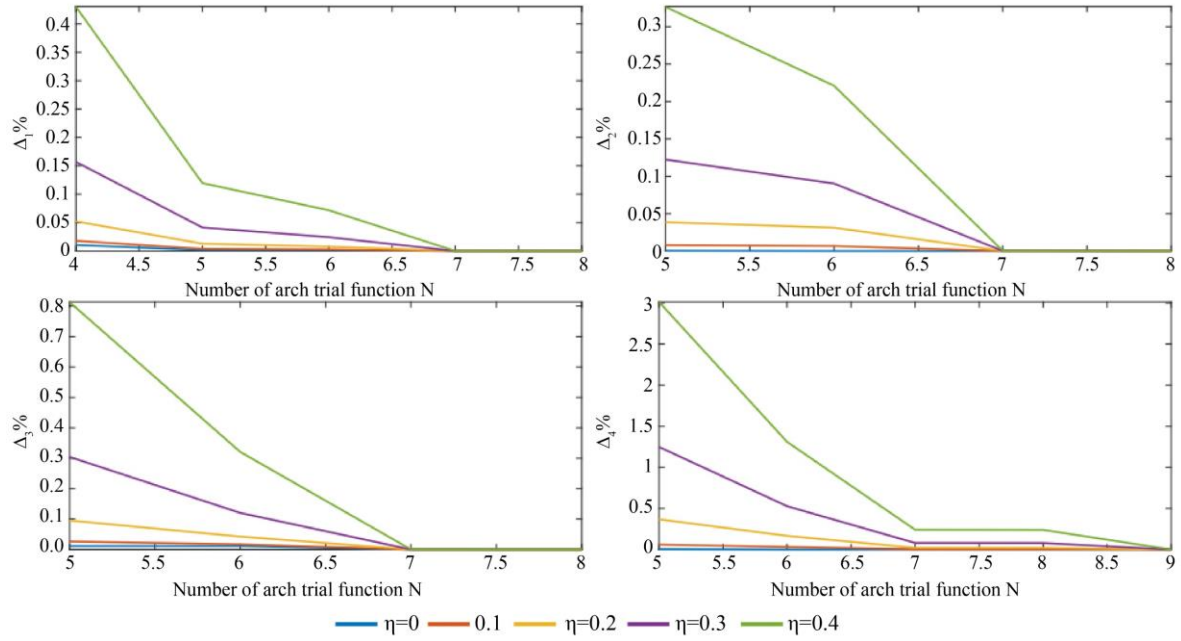

Fig. 5 Convergence study for the first four frequency parameters of a tapered 120°CC circular arc

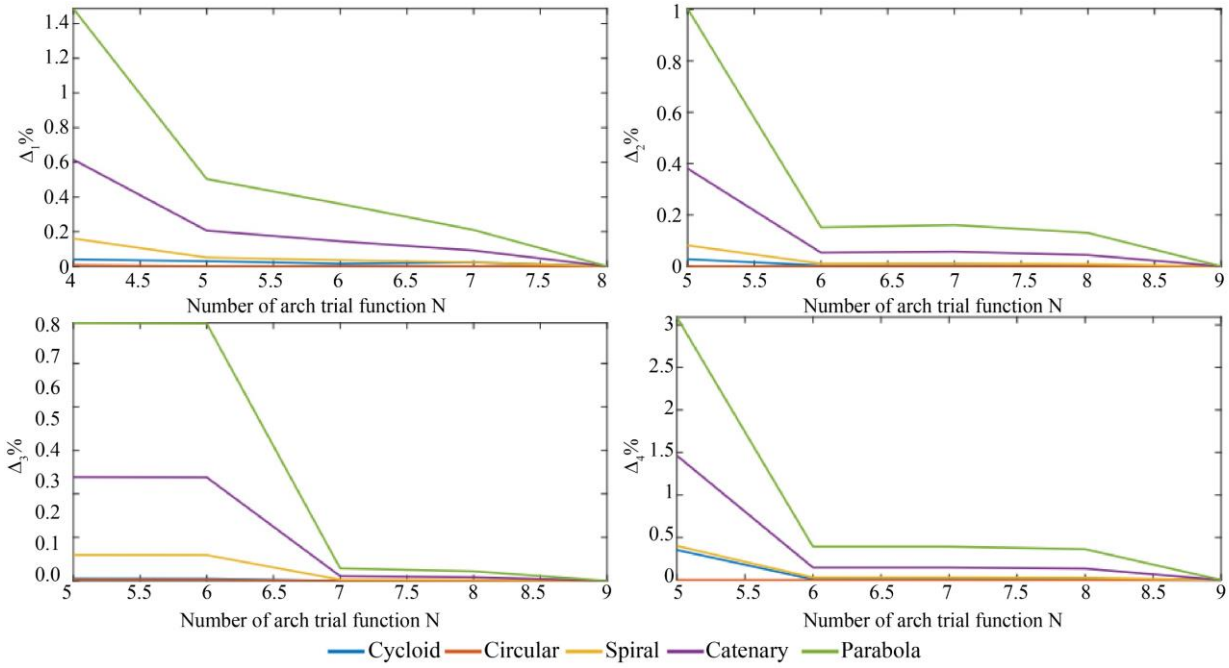

Fig. 6 Convergence study for the first four frequency parameters of 60°CC curved

Table 4. First eight frequency parameters Ω_i and their contribution coefficients a_i for a 20° CS parabola tapered arc with $\eta = 0.4$.

	Ω_1	Ω_2	Ω_3	Ω_4	Ω_5	Ω_6	Ω_7	Ω_8
	393.193	755.174	1372.983	2045.153	2969.230	4001.288	5400.885	7415.685
a_1	9.86E-01	3.77E-01	1.23E-01	-6.29E-02	1.19E-01	-4.91E-02	-9.37E-02	-1.26E-02
a_2	1.60E-01	-8.62E-01	1.78E-01	-5.40E-03	-6.68E-03	-1.74E-02	1.14E-02	-2.45E-02
a_3	4.39E-02	-3.33E-01	-9.35E-01	-5.09E-01	2.77E-03	-8.16E-03	-3.62E-02	4.37E-03
a_4	7.61E-03	-5.69E-02	-2.56E-01	6.94E-01	3.04E-01	4.37E-02	-1.08E-04	-7.86E-03
a_5	4.53E-03	-3.27E-02	-1.12E-01	4.89E-01	-8.62E-01	-6.04E-01	6.74E-02	7.42E-03
a_6	9.55E-04	-6.44E-03	-2.34E-02	1.08E-01	-3.39E-01	5.67E-01	-3.48E-01	5.75E-02
a_7	7.94E-04	-5.29E-03	-1.42E-02	6.43E-02	-1.85E-01	5.46E-01	8.80E-01	-5.52E-01
a_8	1.20E-04	-7.28E-04	-2.38E-03	9.95E-03	-3.32E-02	1.05E-01	3.00E-01	8.31E-01

Table 5. First two frequency parameters $\Omega_{1,2}$ for CC symmetric tapered circular arches η=0,1. (Case 1)

	Present	**ES [27]**	**RRM[3]**	**CDM[20]**	**GDQR[20]**	**DQM[15]**
θ°	Fundamental Frequency Parameter Ω_1					
10	2149.7606	2149.7316	2034	2138.3	2149.7593	2149.7594
20	535.4505	535.4431	506.54	532.59	535.45	535.45
30	236.5185	236.5152	223.7	235.26	236.5183	236.5183
40	131.9089	131.9070	124.73	131.2	131.9088	131.9088
50	83.5074	83.50616			83.5073	83.5073
θ°	Second Frequency Parameter Ω_2					
10	3859.2687	3859.201	3859.9	3821.7	3859.2373	3858.7878
20	963.4396	963.4217	963.59	954.09	963.4309	963.4028
30	427.1773	427.1692	427.24	422.92	427.1733	427.1678
40	239.4889	239.4843	239.52	237.17	239.4866	239.4849
50	152.6196	152.6167			152.6181	152.6174

Table 6. The First frequency parameter Ω_1 of a SS asymmetric tapered circular arc η=0,1.(Case 2)

θ°	**Present**	**ES[27]**	**RRM[3]**	**FEM[3]**	**CDM[20]**	**GDQM[20]**	**QM[15]**	**DTM[24]**	**GDQ[24]**
10	1290.4855	1290.48392	1286.5		1287.8	1290.485	1290.485	1290.5	1290.5
20	320.7633	320.762901	319.09	320.81	320.11	320.7631	320.7631	320.76	320.76
30	141.2012	141.201091		141.05	140.92	141.2012		141.2	141.2
40	78.3731	78.3730359	78.069	78.438	78.22	78.3731	78.3731	78.323	78.323
50	49.3123	49.3122615	49.124		49.218	49.3123		49.312	49.312
60	33.5460	33.5460425	33.43	33.621	33.484	33.5461	33.5461	33.546	33.546
80	17.9206	17.9206083				17.9206	17.9206		

4. Results Validation

The first arc investigated is a circular symmetrical CC arc depicted in Figure 5(a) (case 1), with a taper ratio $\eta = 0.1$. The first two frequency parameters $\Omega = R_0^2\sqrt{\frac{\mu S_0}{EI_0}}\omega$ are listed in Table 5 and compared to those in the bibliography. It should be noted that the current results are very similar to those obtained by other methods, such as the generalized differential quadrature rule (GDQR) developed by Liu [13] and the differential quadrature method (DQM) investigated by Karami [14], the difference percentages are very small and do not exceed $4 \times 10^{-4}\%$. Moreover, the difference percentages between the present results and those found by the so-called Cell Discretization Method (CDM) [13] remain less than 0.99%it is well known that the CDM and RRM predict a lower and upper bound respectively to the exact solution. The results found by Tufekci [16] are accurate enough, but the results found using RRM [24] present different percentages that reach 5% compared to the rest of the results in Table 5. This is explained by the trial arc functions, which are polynomial approximations. Thanks to the good choice of the trial arc functions used in the present Rayleigh-Ritz formulation, the results found here are the most accurate of those given by the other research based on the RRM. Table 6 gives the fundamental frequency parameters Ω_1 of an asymmetric circular SS arc (Figure 5(c)), the height variation function is $h(\alpha^*) = (1 + \eta(2\alpha^* - 1))$ (case 2), and the taper ratio is $\eta = 0.1$. An excellent agreement with the results listed in this table is noticed; again, the results found using the Rayleigh-Ritz method by Laura [3] are less accurate than another method in this table.

The first two frequency parameters $\Omega_{1,2}$ of tapered symmetric SS and CC circular arches shown in Figure 5(b) with varying cross-sections represented by the sin function (case 5) with two values of the taper ratio $\eta = 0{,}1$ are summarized in Table 7. This later table compares the present results to those by Shin [24], who have used two methods, the Differential Transformation Method (DTM) and the Generalized Differential Quadrature Method (GDQM). Again, an excellent agreement with all results presented in this table.

The comparison with the same references is given in Table 8 for a symmetric SS arc plotted in Figure 5(b) with varying sections represented by the quadratic function $h_4(\alpha^*) = (1 + \eta(2\alpha^* - 1))^2$ for $0 < \alpha^* < 1$ (Case 4). The present comparison is also excellent. Table 9 lists the fundamental frequency parameter Ω_1 of a circular CC arc with several values of tapered ratios η.

Two sets of results are presented in this table: the first one is about an asymmetric CC arc shown in Figure 6(d) with a linear variable thickness according to the function h_2, the fundamental frequency parameters for opening angles $\theta = 10°, 20°, 40°, 60°, 80°$ and tapered ratio $\eta = 0.1,0.2,0.3,0.4$are compared to those found by Karami (DQM) [15] and Lui (GDQR) [20]. The differences in percentage between the present results and those of Refs [15] and [20] remain less 0.0045%. The second set of results compares the fundamental frequency parameter of a symmetrical CC arc shown in Figure 5(a) having a linear variable thickness according to the function $h_1$with the results given by author for opening angles $\theta = 20°, 30°, 40°, 50°$ and tapered ratio $\eta = 0,0.1,0.2,0.3$. Even though they are very close to each other, the results of this work are more accurate than those given by an author because the results corresponding to $\eta = 0$ those given by De Rosa [10] (DQM) are identical to those given by this work.

Table 7. First two frequency parameters $\Omega_{1,2}$ of SS and CC symmetric tapered circular arc η=0,1. (Case 5)

		Fundamental frequency parameter					Second frequency parameter			
	$\theta°$	Present	ES[27]	DTM[24]	GDQM[24]		Present	ES[27]	DTM [24]	GDQM[22]
SS	10	2127.1342	2127.716	2127.1	2127.1		3816.4893	3823.409	3816.5	3816.5
	20	529.8201	529.9307	529.82	529.82		952.7674	954.4785	952.76	952.76
	30	234.0355	234.0592	234.04	234.04		422.4511	423.198	422.45	422.45
	40	130.5273	130.5212	130.53	30.53		236.8437	237.2532	236.84	236.84
	50	82.6354	82.616	82.635	82.635		150.9376	151.191	150.94	150.94
	60	56.6380	56.61197	56.638	56.638		104.2764	104.4451	104.28	104.28
CC	01	1333.8494		1333.8	1333.8		2874.7293		2874.8	2874.8
	20	331.5784		331.58	331.58		717.2857		717.3	717.3
	30	145.9884		145.99	145.99		317.7622		317.77	317.77
	40	81.0501		81.05	81.05		177.9327		177.94	177.94
	50	51.0122		51.012	51.012		113.2157		113.22	113.22
	60	34.7148		34.715	34.715		78.0650		78.067	78.067

Table 8. First two frequency parameters $\Omega_{1,2}$ of an SS symmetric tapered circular arc η=0,1. (Case 4)

	Fundamental frequency parameter				Second frequency parameter			
	Present	ES[27]	DTM[24]	GDQM[24]	Present	ES[24]	DTM[24]	GDQM[24]
10	1285.1103	1285.106	1285.1	1285.1	2750.3173	2750.391	2750.4	2750.4
20	319.4265	319.4256	319.43	319.43	686.2288	686.2475	686.25	686.25
30	140.6123	140.6119	140.61	140.61	303.9934	304.0019	304	304
40	78.0457	78.04555	78.046	78.046	170.2146	170.2196	170.22	170.22
50	49.1059	49.1058	49.106	49.106	108.2981	108.3014	108.3	108.3
60	33.4052	33.40521	33.405	33.405	74.6686	74.67106	74.671	74.671

Table 9. The fundamental frequency parameter Ω_1 of a CC tapered circular arc with several values of tapered ratio η

		A CC asymmetric arc : h_2 (Case 2)				
		$\theta = 10°$	20°	40°	60°	80°
$\eta = 0.1$	Present	2016.998	502.3076	123.6710	53.6080	29.1459
	Ref [15]	2016.983	502.3033	123.6698	53.6074	29.1456
	Ref [20]	2016.983	502.3033	123.6698	53.6075	29.1456
$\eta = 0.2$	Present	2001.871	498.5421	122.7450	53.2074	28.9288
	Ref [15]	2001.812	498.5259	122.7406	53.2053	28.9275
	Ref [20]	2001.813	498.526	122.7406	53.2053	28.9275
$\eta = 0.3$	Present	1976.206	492.1548	121.1744	52.5280	28.5605
	*Ref [15]	1975.993	492.0976	121.1591	52.5208	28.5564
	Ref [20]	1975.996	492.0978	121.1592	52.5209	28.5564
$\eta = 0.4$	Present	1939.330	482.9810	118.9195	51.5528	28.0322
	Ref [15]	1938.632	482.7954	118.8708	51.5304	28.0193
	Ref [20]	1938.637	482.7959	118.8708	51.5305	28.0193
		A CC symmetric arc h_1 (Case 1)				
		$\theta = 20°$	30°	40°	50°	
$\eta = 0$	Present	503.55	222.37	123.98	78.45	
	Ref [10]	503.55	-	123.98	-	
	Ref [28]	504.11	223.11	124.97	79.78	
$\eta = 0.1$	Present	535.45	236.52	131.91	83.51	
	Ref [28]	536.02	237.24	132.86	84.76	
		538.95	238.07	132.78	84.06	
$\eta = 0.2$	Present	566.82	250.43	139.71	88.48	
	Ref [28]	567.39	251.13	140.62	89.67	
	Ref [27]	568.3	251.09	140.08	88.72	
$\eta = 0.3$	Present	597.73	264.14	147.40	93.38	
	Ref [28]	598.04	264.82	148.28	94.51	
	Ref [27]	597.3	263.95	147.29	93.32	

The results concerning the fundamental frequency parameters $\widetilde{\Omega}_1 = \sqrt{\frac{\mu S_0}{EI_0}}(R_0\theta)^2\omega_1$ of tapered asymmetric CC and CS tapered arches with variable curvature are listed in Table 10 for tapered ratios $\eta = 0.1,0.2,0.3,0.4$ and opening angles $\theta = 10°, 20°, 30°, 40°, 50°, 60°$. The CC, SC tapered arc shown in Figures 5(d) and 5(c) have Varying cross-sections according to the function $h_2(\alpha^*) = 1 + \eta(2\alpha^* - 1)$ and $h_3(\alpha^*) = 1 - \eta(2\alpha^* - 1)$ respectively. The results are very close to those given by Gutierrez [14] who has used polynomial coordinate functions and the Ritz method. The strong point of the present method, in accordance with that of Gutierrez, is that the present Rayleigh-Ritz method does not diverge.

Table 10. The fundamental frequency parameter $\widetilde{\Omega}_1$ of a CC and CS asymmetric tapered arc with variable curvature

			CC arc (Case 2: $h2(\alpha^*) = 1 + \eta(2\alpha^* - 1)$)					SC arc (Case 3 : $h3(\alpha^*) = 1 - \eta(2\alpha^* - 1)$)			
	θ		η = 0.1	η = 0.2	η = 0.3	η = 0.4		η = 0.1	η = 0.2	η = 0.3	η = 0.4
Parabola	10	(a)	60.97	60.52	59.74	58.63		48.69	47.86	46.77	45.42
		(b)	60.53	60.46	59.73	58.37		48.49	47.74	46.46	45.34
	20	(a)	59.35	58.90	58.15	57.06		47.35	46.53	45.48	44.16
		(b)	59.05	58.85	58.10	56.78		47.15	46.47	45.43	44.09
	30	(a)	56.69	56.26	55.54	54.51		45.15	44.37	43.36	42.10
		(b)	56.49	56.41	55.42	54.11		45.07	44.36	43.26	41.85
	40	(a)	53.07	52.67	52.00	51.04		42.17	41.44	40.49	39.31
		(b)	52.91	52.65	51.76	50.43		42.14	41.28	40.29	38.88
	50	(a)	48.61	48.25	47.64	46.78		38.52	37.85	36.98	35.90
		(b)	48.41	4.08	47.15	46.14		38.26	37.52	36.55	35.32
	60	(a)	43.46	43.14	42.61	41.87		34.31	33.71	32.94	31.98
		(b)	42.98	42.70	41.85	40.86		33.70	32.98	32.00	30.05
Catenary	10	(a)	61.13	60.67	59.89	58.78		48.82	47.98	46.89	45.54
		(b)	60.59	60.59	59.93	58.65		48.58	47.91	46.81	45.43
	20	(a)	59.96	59.51	58.75	57.66		47.84	47.02	45.95	44.61
		(b)	59.59	59.46	58.78	57.41		47.66	46.90	45.95	44.45
	30	(a)	58.04	57.61	56.87	55.81		46.23	45.43	44.40	43.10
		(b)	57.75	57.55	56.85	55.49		46.04	45.34	44.36	42.89
	40	(a)	55.41	54.99	54.29	53.28		44.04	43.27	42.27	41.04
		(b)	55.20	54.99	54.18	52.83		44.00	43.17	42.14	40.79
	50	(a)	52.11	51.72	51.06	50.12		41.30	40.57	39.63	38.47
		(b)	52.00	51.69	50.75	49.55		41.18	40.39	39.39	38.05
	60	(a)	48.22	47.86	47.26	46.41		38.09	37.41	36.54	35.45
		(b)	48.08	47.66	46.81	45.78		37.83	37.09	36.11	34.87
Spiral	10	(a)	61.29	60.83	60.05	58.93		48.94	48.10	47.01	45.65
		(b)	60.79	60.79	60.13	58.78		48.74	48.00	46.98	45.51
	20	(a)	60.58	60.13	59.36	58.25		48.34	47.50	46.42	45.08
		(b)	60.13	60.06	59.33	58.10		48.16	47.41	46.30	44.98
	30	(a)	59.42	58.97	58.22	57.13		47.33	46.51	45.45	44.12
		(b)	58.99	58.92	58.24	56.85		47.15	46.39	45.43	43.90
	40	(a)	57.81	57.38	56.64	55.59		45.95	45.15	44.10	42.81
		(b)	57.55	57.41	56.56	55.20		45.86	45.07	44.00	42.61
	50	(a)	55.77	55.36	54.65	53.64		44.21	43.43	42.41	41.16
		(b)	55.57	55.35	54.55	53.21		44.09	43.26	42.30	40.98
	60	(a)	53.33	52.93	52.26	51.30		42.14	41.38	40.40	39.19
		(b)	53.21	52.92	52.07	50.83		42.04	41.18	40.42	38.88
Circle	10	(a)	61.44	60.98	60.20	59.08		49.07	48.23	47.13	45.77
		(b)	60.92	60.92	60.26	58.92		48.82	48.08	47.07	45.69
	20	(a)	61.20	60.75	59.97	58.85		48.84	47.99	46.90	45.54
		(b)	60.72	60.66	60.00	58.65		48.58	47.83	46.81	45.43
	30	(a)	60.81	60.36	59.59	58.48		48.45	47.61	46.52	45.16
		(b)	60.33	60.26	59.59	58.31		48.24	47.49	46.47	45.07
	40	(a)	60.28	59.82	59.06	57.96		47.92	47.08	45.99	44.63
		(b)	59.80	59.73	59.05	57.82		47.74	46.90	45.95	44.54
	50	(a)	59.60	59.15	58.40	57.31		47.26	46.41	45.32	43.97
		(b)	59.12	59.05	58.37	57.13		47.07	46.21	45.25	43.81
	60	(a)	58.79	58.35	57.60	56.53		46.47	45.62	44.53	43.19
		(b)	58.31	58.24	57.68	56.35		46.21	45.51	44.54	43.08

	10	(a)	61.60	61.14	60.35	59.23		49.19	48.35	47.25	45.89
Cycloid		(b)	61.05	61.05	60.39	59.05		48.90	48.24	47.15	45.78
	20	(a)	61.83	61.37	60.58	59.45		49.34	48.49	47.38	46.01
		(b)	61.35	61.25	60.66	59.33		49.07	48.33	47.32	45.95
	30	(a)	62.23	61.76	60.97	59.84		49.59	48.72	47.60	46.21
		(b)	61.57	61.57	61.05	59.80		49.31	48.49	47.49	46.13
	40	(a)	62.81	62.34	61.54	60.40		49.95	49.07	47.93	46.51
		(b)	62.03	62.16	61.54	60.46		49.55	48.82	47.91	46.47
	50	(a)	63.58	63.11	62.30	61.14		50.44	49.53	48.36	46.92
		(b)	62.54	62.86	62.48	61.31		49.96	49.23	48.24	46.81
	60	(a)	64.58	64.10	63.28	62.11		51.08	50.14	48.94	47.46
		(b)	63.30	63.62	63.56	62.41		50.35	49.71	48.74	47.49

(a) values of this work, (b) values of Ref [8]

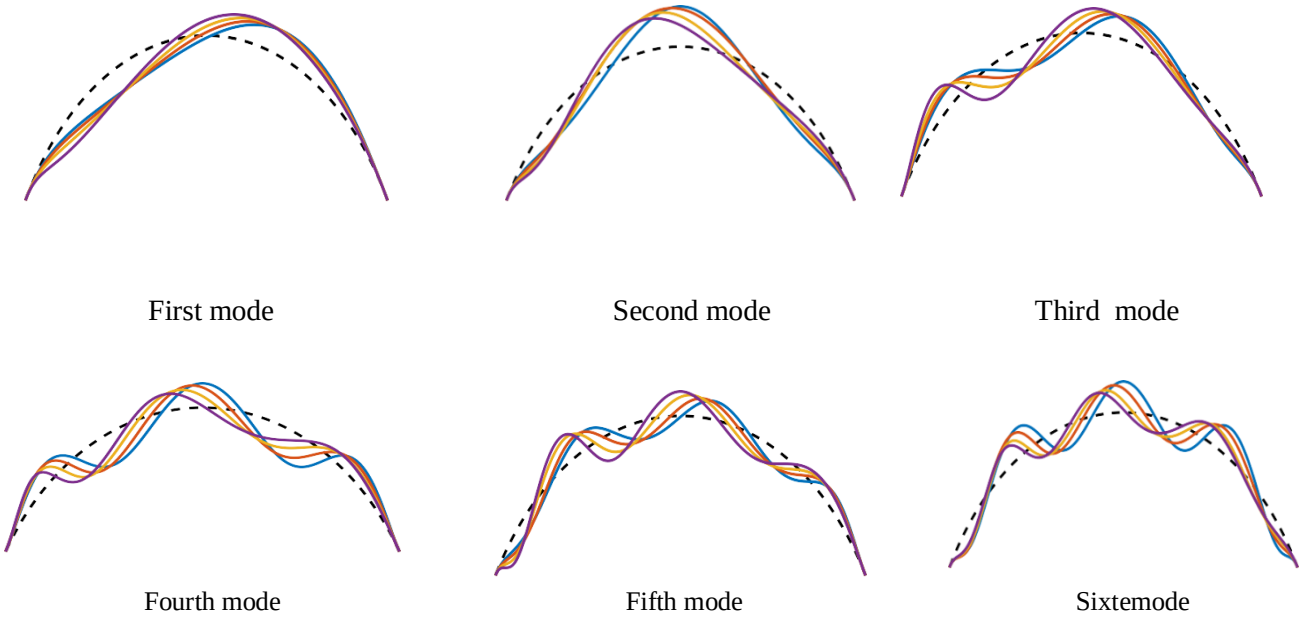

Fig. 7 The lowest six normalized mode shapes of 120° tapered CC circular arches with various tapered ratios η = 0, 0.2, 0.4, 0.6. Dashed black lines represent arc before deformation.

Figure 7 plots the lowest six normalized mode shapes of a 120° tapered CC circular asymmetric arc with various tapered ratios $\eta = 0,0.2,0.4,0.6$; the variation law of the section height is given by the function h_2 defined above. The dashed black line presents an arc before deformation, and the blue, orange, yellow and pulp curves correspond to arc modes corresponding to tapered ratios $= 0,0.2,0.4,0.6$, respectively. For all the modes and whatever the value of the tapered ratio η, the slopes at the ends are zero because the arc is clamped at both ends. It is quite clear that the circular arc with constant section ($\eta = 0$), whose modes are represented by the blue curves, is a symmetrical arc; therefore, the odd modes are asymmetrical, and the even modes are symmetrical. On the other hand, $\eta \neq 0$i.e. when the arc has a variable section, the odd modes are no longer asymmetrical, and the even modes are no longer symmetrical. It is concluded that the taper ratio has a significant influence on the modes.

5. Conclusion

This paper sounds quite comprehensive in its treatment of the Rayleigh-Ritz method for analyzing free vibrations of inextensible thin tapered arches with variable radii. The use of particular solutions of the governing differential equation for circular arcs with uniform cross-sections as trial arc functions, determined through symbolic and numerical calculations via MATLAB, is a robust approach. It is interesting to note the consideration of various end conditions and arc geometries, including parabolic, cycloid, catenary, circular, and spiral arcs, each with different cross-

section variations. The sensitivity of the convergence study to the tapered ratio indicates the importance of carefully considering this parameter in the analysis. The observation that frequency parameters are generally insensitive to arc geometry but influenced by the taper and opening angle underscores the complexity of the system under study. The differing behavior of frequency parameters for spiral arcs compared to others adds an intriguing dimension to the findings.

The impact of cross-section taper on mode shapes suggests that the geometry of the arch plays a significant role in determining its vibrational characteristics.Overall, the assertion that the Rayleigh-Ritz formulation presented in the paper is the most accurate compared to previous studies using the same method is a strong claim, indicating the potential for this approach to be applied to a wide range of arch structures, including those made of functionally graded materials or carrying added masses.

References

[1] Byoung Koo Lee et al., "Free Vibrations of Tapered Horseshoe Circular Arch with Constant Volume," *Applied Sciences*, vol. 10, no. 16, pp. 1-13, 2020. [CrossRef] [Google Scholar] [Publisher Link]

[2] Desmond Adair, and Martin Jaeger, "In-plane Free Vibration Analysis of a Scimitar-Type Rotating Curved Beam Using the Adomian Modified Decomposition Method," *Mathematical and Computational Applications*, vol. 25, no. 4, pp. 1-18, 2020. [CrossRef] [Google Scholar] [Publisher Link]

[3] P.L. Verniere de Irassar, and P.A.A. Laura, "A Note on the Analysis of the First Symmetric Mode of Vibration of Circular Arches of Non-Uniform Cross-Section," *Journal of Sound and Vibration*, vol. 116, no. 3, pp. 580-584, 1987. [CrossRef] [Google Scholar] [Publisher Link]

[4] J.A. Reyes, R.E. Rossi, and P.A.A. Laura, "Numerical Experiments on Rayleigh's Optimization Method when Applied to Beam Vibrations Studied by Means of the Finite Element Method," *Journal of Sound and Vibration*, vol. 117, no. 3, pp. 583-587, 1987. [CrossRef] [Google Scholar] [Publisher Link]

[5] P.A.A. Laura, and P.L. Verniere de Irassar, "A Note on In-Plane Vibrations of Arch-Type Structures of Non-Uniform Cross-Section: The Case of Linearly Varying Thickness," *Journal of Sound and Vibration*, vol. 124, no. 1, pp. 1-12, 1988. [CrossRef] [Google Scholar] [Publisher Link]

[6] E. Romanelli, and P.A. Laura, "Fundamental Frequencies of Non-Circular, Elastic, Hinged Arcs," *Journal of Sound and Vibration*, vol. 24, no. 1, pp. 17-22, 1972. [CrossRef] [Google Scholar] [Publisher Link]

[7] T.M. Wang, and J.A. Moore, "Lowest Natural Extensional Frequency of Clamped Elliptic Arcs," *Journal of Sound and Vibration*, vol. 30, no. 1, pp. 1-7, 1973. [CrossRef] [Google Scholar] [Publisher Link]

[8] R.H. Gutierrez et al., "In-Plane Vibrations of Non-Circular Arcs of Non-Uniform Cross-Section," *Journal of Sound and Vibration*, vol. 129, no. 2, pp. 181-200, 1989. [CrossRef] [Google Scholar] [Publisher Link]

[9] R.E. Rossi, P.A.A. Laura, and P.L. Verniere de Irassar, "In-Plane Vibrations of Cantilevered Non-Circular Arcs of Non-Uniform Cross Section with a Tip Mass," *Journal of Sound and Vibration*, vol. 129, no. 2, pp. 201-213, 1989. [CrossRef] [Google Scholar] [Publisher Link]

[10] C.S. Huang et al., "An Exact Solution for In-Plane Vibrations of an Arch having Variable Curvature and Cross Section," *International Journal of Mechanical Sciences*, vol. 40, no. 11, pp. 1159-1173, 1998. [CrossRef] [Google Scholar] [Publisher Link]

[11] X. Tong, N. Mrad, and B. Tabarrok, "In-Plane Vibration of Circular Arches with Variable Cross-Sections," *Journal of Sound and Vibration*, vol. 212, no. 1, pp. 121-140, 1998. [CrossRef] [Google Scholar] [Publisher Link]

[12] Byoung Koo Lee et al., "Free Vibration Analysis of Parabolic Arches in Cartesian Coordinates," *International Journal of Structural Stability and Dynamics*, vol. 3, no. 3, pp. 377-390, 2003. [CrossRef] [Google Scholar] [Publisher Link]

[13] G.R. Liu, and T.Y. Wu, "In-Plane Vibration Analyses of Circular Arches by the Generalized Differential Quadrature Rule," *International Journal of Mechanical Sciences*, vol. 43, no. 11, pp. 2597-2611, 2001. [CrossRef] [Google Scholar] [Publisher Link]

[14] G. Karami, and P. Malekzadeh, "In-Plane Free Vibration Analysis of Circular Arches with Varying Cross-Sections Using Differential Quadrature Method," *Journal of Sound and Vibration*, vol. 274, no. 3-5, pp. 777-799, 2004. [CrossRef] [Google Scholar] [Publisher Link]

[15] Young-Jae Shin, Kyunng-Mun Kwon, and Jong-Hak Yun, "Vibration Analysis of a Circular Arch with Variable Cross-Section Using Differential Transformation and Generalized Differential Quadrature," *Journal of Sound and Vibration*, vol. 309, no. 1-2, pp. 9-19, 2008. [CrossRef] [Google Scholar] [Publisher Link]

[16] Ekrem Tufekci, and Oznur Ozdemirci Yigit, "In-Plane Vibration of Circular Arches with Varying Cross-Sections," *International Journal of Structural Stability and Dynamics*, vol. 13, no. 1, 2013. [CrossRef] [Google Scholar] [Publisher Link]

[17] G.C. Tsiatas, and M. Fragiadakis, "Dynamic Analysis and Seismic Response of Planar Circular Arches with Variable Cross-Section," *Journal of Earthquake Engineering*, vol. 22, no. 2, pp. 191-210, 2018. [CrossRef] [Google Scholar] [Publisher Link]

[18] Ahmad Reshad Noori, Timucin Alp Aslan, and Beytullah Temel, "An Efficient Approach for Inplane Free and Forced Vibrations of Axially Functionally Graded Parabolic Arches with Nonuniform Cross Section," *Composite Structures*, vol. 200, pp. 701-710, 2018. [CrossRef] [Google Scholar] [Publisher Link]

[19] Qingbo Wang, Zhongmin Wang, and Ting Chen, "In-Plane Free Vibration of Inhomogeneous Curved Beam with Variable Curvature Under Elastic Constraints," *Journal of Vibration Engineering & Technologies*, vol. 11, no. 2, pp. 739-754, 2022. [CrossRef] [Google Scholar] [Publisher Link]

[20] J. Melchiorre et al., "Differential Formulation and Numerical Solution for Elastic Arches with Variable Curvature and Tapered Cross-Sections," *European Journal of Mechanics - A/Solids*, vol. 97, 2023. [CrossRef] [Google Scholar] [Publisher Link]

[21] P.A.A. Laura et al., "A Note on Vibrations of a Circumferential arch with Thickness Varying in a Discontinuous Fashion," *Journal of Sound and Vibration*, vol. 120, no. 1, pp. 95-105, 1988. [CrossRef] [Google Scholar] [Publisher Link]

[22] V.H. Cortinez et al., "Numerical Experiments on Vibrating Cantilever Arches of Varying Cross-Section," *Journal of Sound and Vibration*, vol. 110, no. 2, pp. 356-358, 1986. [CrossRef] [Google Scholar] [Publisher Link]

[23] C.P. Filipich, P.A.A. Laura, and V.H. Cortinez, "In-Plane Vibrations of an Arch of Variable Cross Section Elastically Restrained Against Rotation at One End and Carrying a Concentrated Mass at the Other," *Applied Acoustics*, vol. 21, no. 3, pp. 241-246, 1987. [CrossRef] [Google Scholar] [Publisher Link]

[24] N.M. Auciello, and M.A. De Rosa, "Free Vibrations of Circular Arches: A Review," *Journal of Sound and Vibration*, vol. 176, no. 4, pp. 433-458, 1994. [CrossRef] [Google Scholar] [Publisher Link]

[25] M.A. De Rosa, and C. Franciosi, "Exact and Approximate Dynamic Analysis of Circular Arches Using DQM," *International Journal of Solids and Structures*, vol. 37, no. 8, pp. 1103-1117, 2000. [CrossRef] [Google Scholar] [Publisher Link]

[26] A.K. Igor, and I.L. Olga, *Formulas Structural Dynamics*, McGraw-Hill, 2001. [Google Scholar]

[27] Ahmed Babahammou, and Rhali Benamar, "The Efficiency of the Rayleigh-ritz Method Applied to In-Plane Vibrations of Circular Arches Elastically Restrained at the Two Ends and Supporting Point Masses," *Advances in Acoustics and Vibration III*, pp. 27-34, 2021. [CrossRef] [Google Scholar] [Publisher Link]

[28] Ahmed Babahammou, and Rhali Benamar, "A Semi Analytical Method for In-Plane Free Vibrations of Arches with a Variable Curvature," *Materials Today: Proceedings*, vol. 59, pp. 893-898, 2022. [CrossRef] [Google Scholar] [Publisher Link]